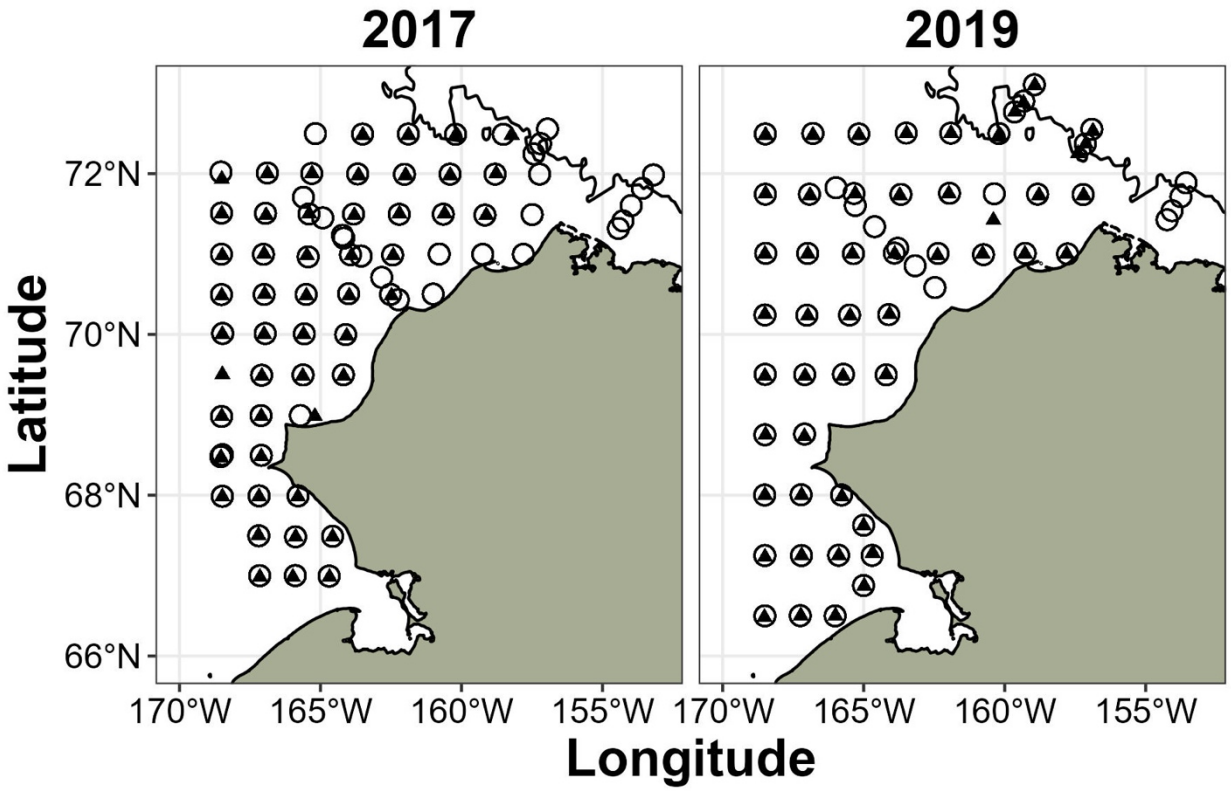

Figure S1. Map of Arctic stations sampled in 2017 and 2019 with an oblique towed bongo net (20 cm, 153 µm) (open circles) and vertically towed Juday net (37 cm diameter, 168 µm mesh) (closed triangles).

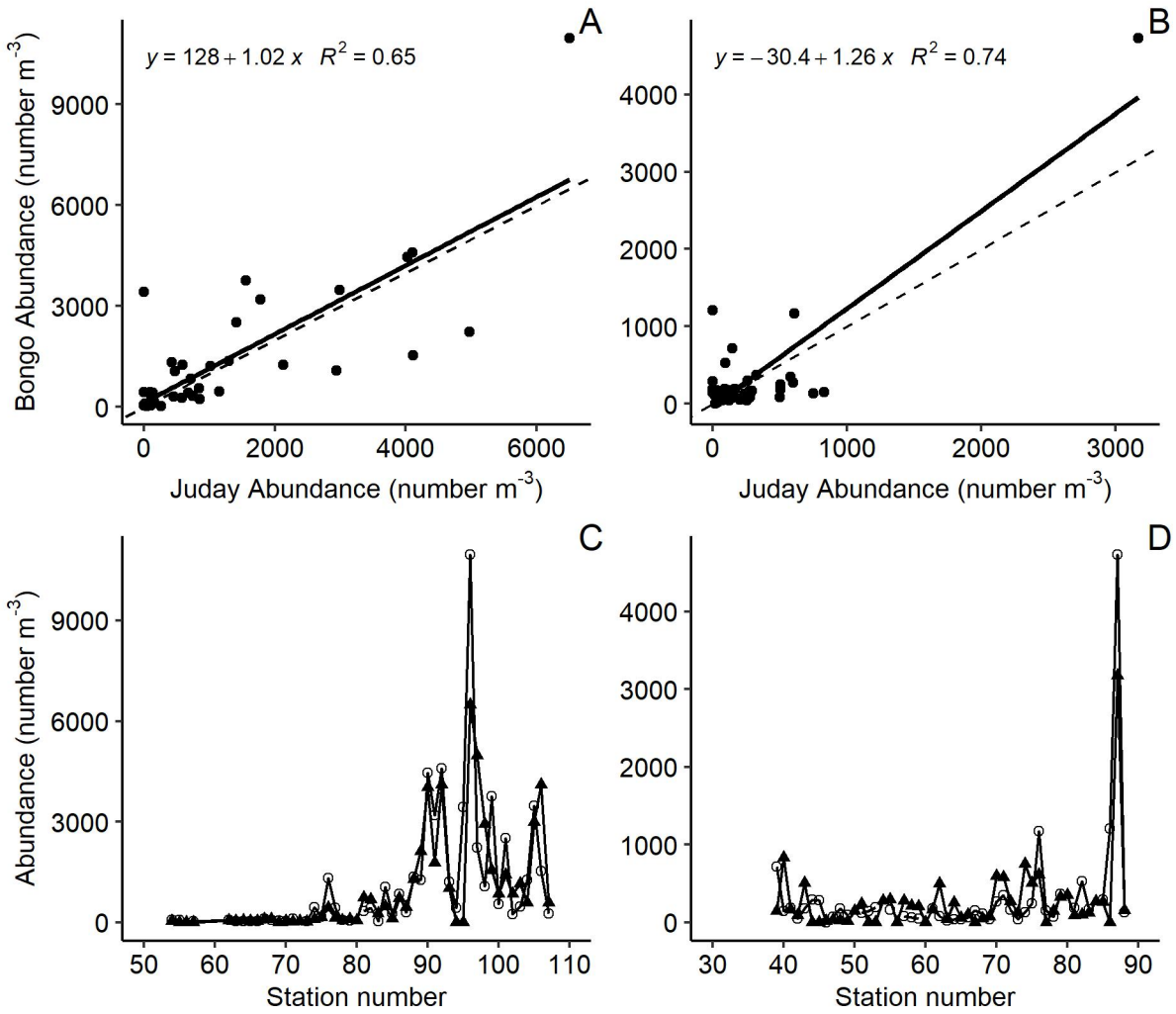

Figure S2. Comparison of *Acartia* spp. abundances between Juday and bongo nets. Linear regression fit (solid line) between the bongo and Juday net abundances for 2017 (A) and 2019 (B). Dashed line is the 1:1 line. Comparison of station by station abundances for bongo net (open circles) and vertically towed Juday net (closed triangles).

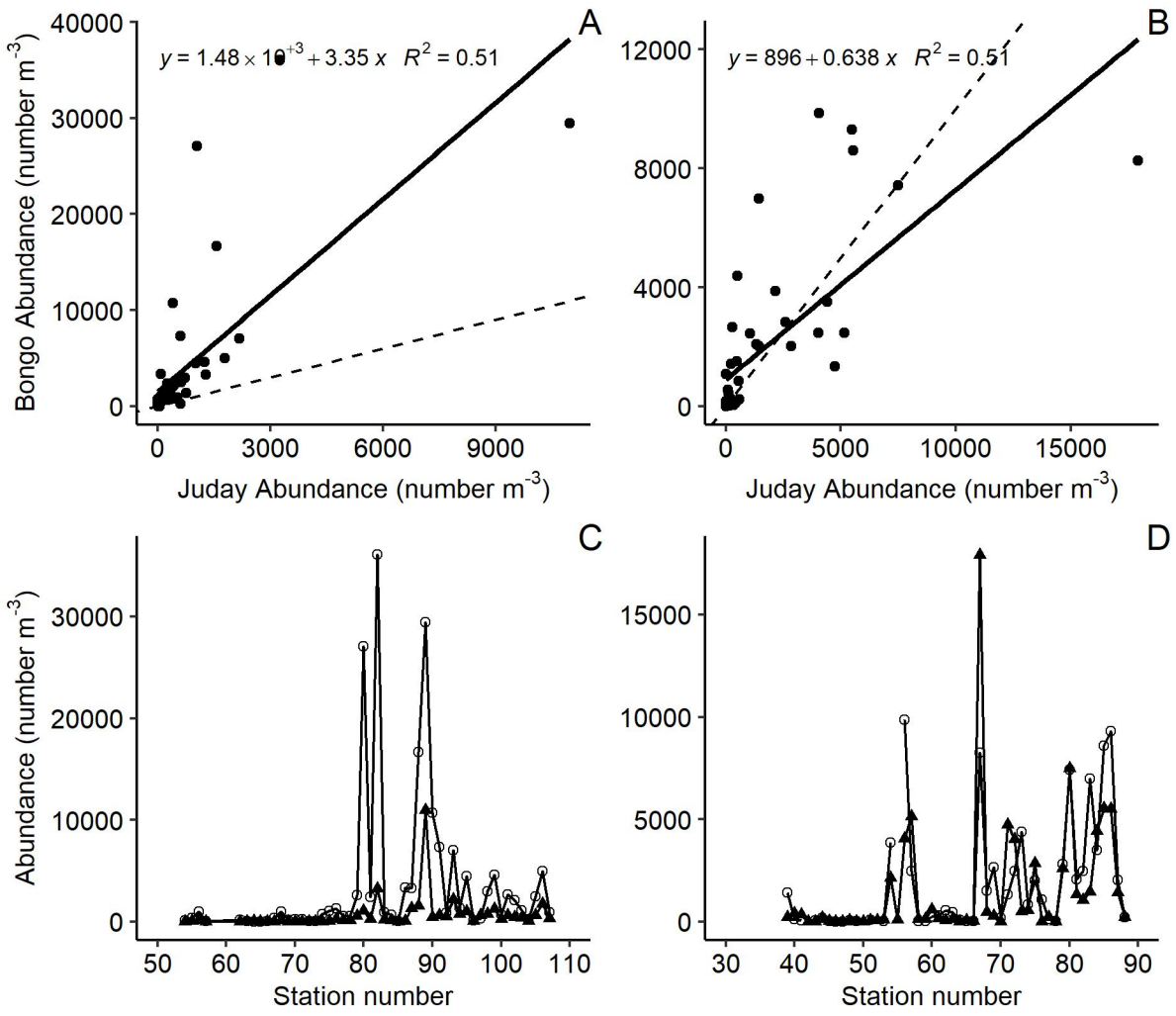

Figure S3. Comparison of Bivalvia larvae abundances between Juday and bongo nets. Linear regression fit (solid line) between the bongo and Juday net abundances for 2017 (A) and 2019 (B). Dashed line is the 1:1 line. Comparison of station by station abundances for bongo net (open circles) and vertically towed Juday net (closed triangles).

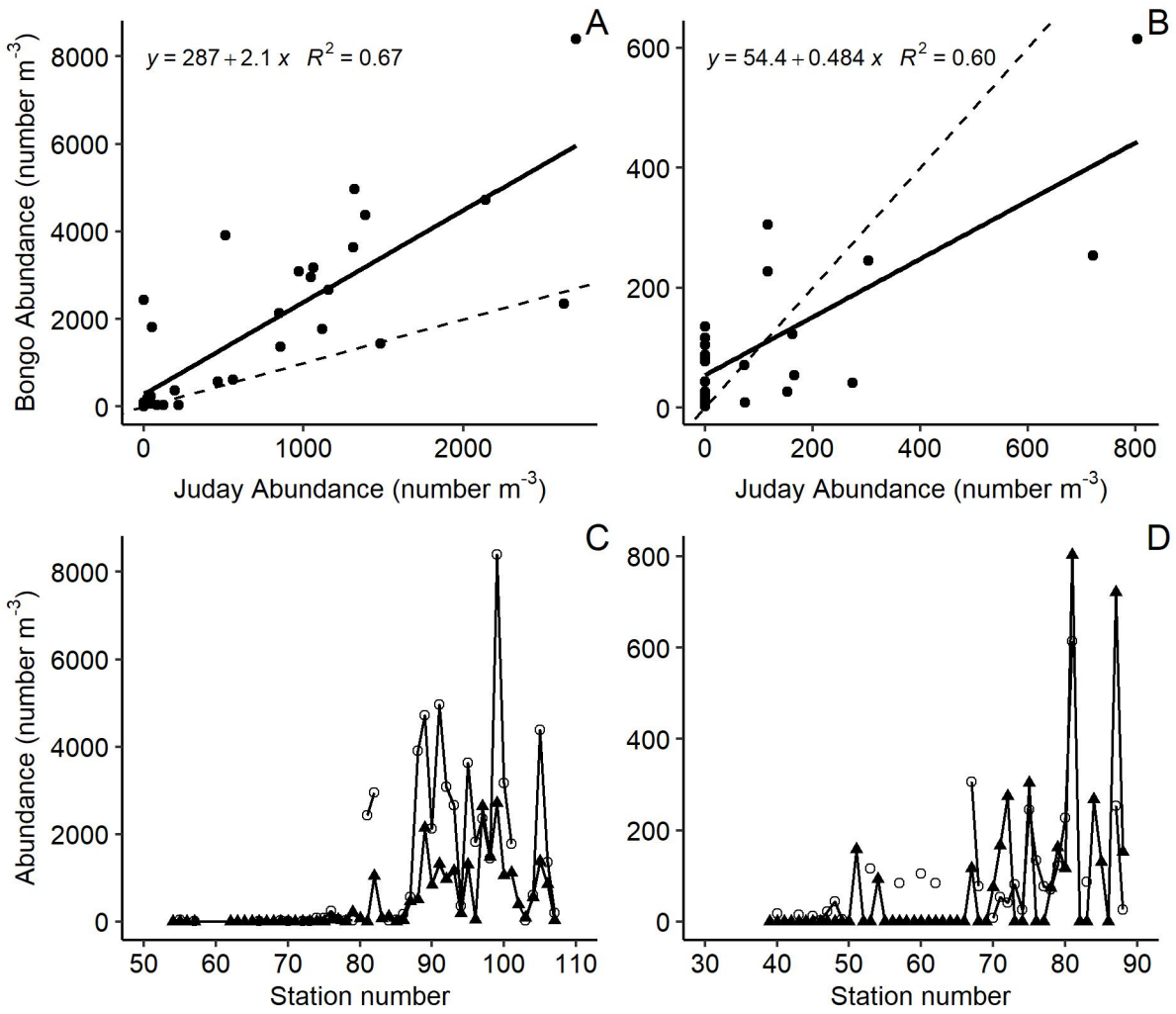

Figure S4. Comparison of *Centropages* spp. abundances between Juday and bongo nets. Linear regression fit (solid line) between the bongo and Juday net abundances for 2017 (A) and 2019 (B). Dashed line is the 1:1 line. Comparison of station by station abundances for bongo net (open circles) and vertically towed Juday net (closed triangles).

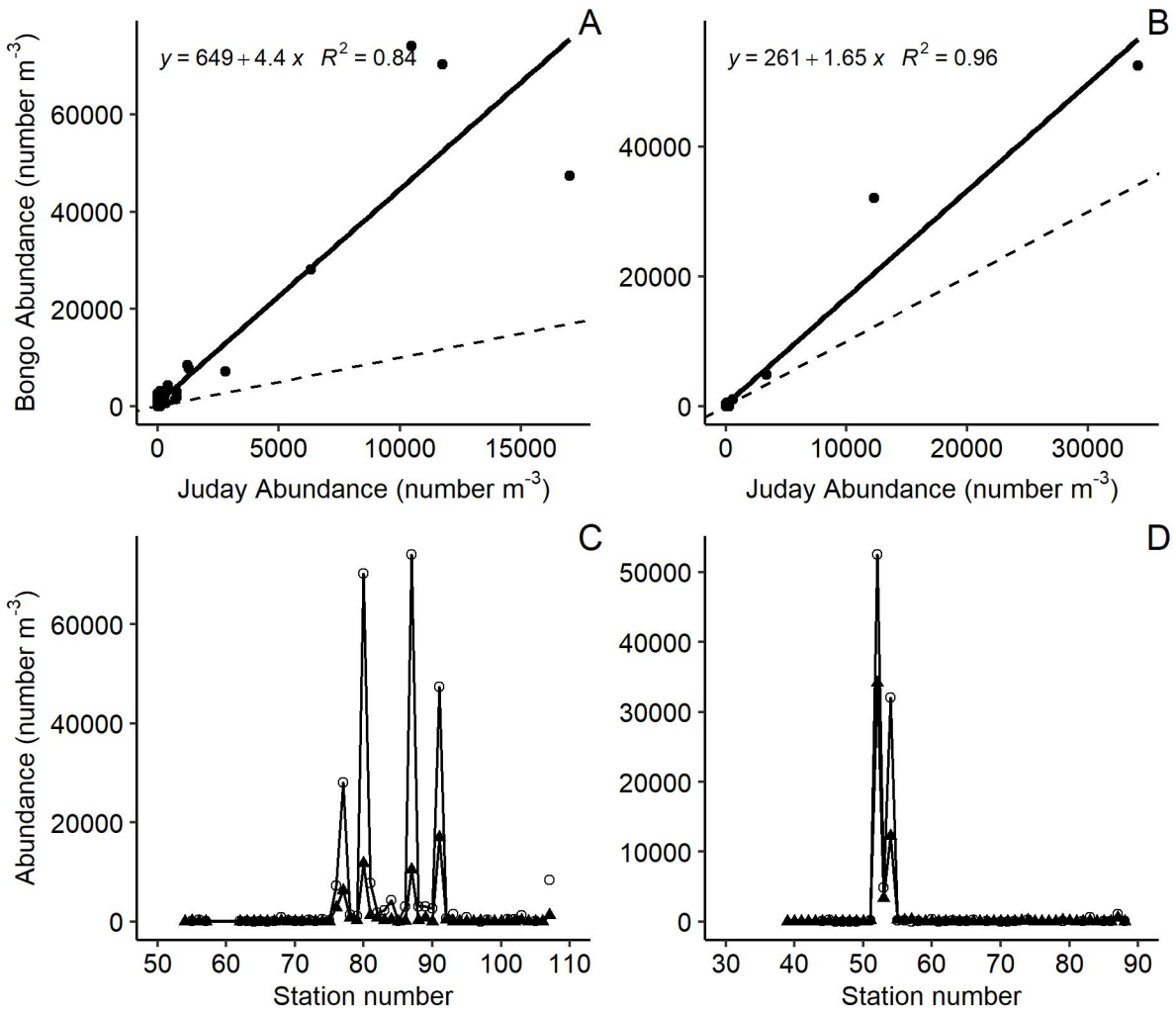

Figure S5. Comparison of Echinodermata larvae abundances between Juday and bongo nets. Linear regression fit (solid line) between the bongo and Juday net abundances for 2017 (A) and 2019 (B). Dashed line is the 1:1 line. Comparison of station by station abundances for bongo net (open circles) and vertically towed Juday net (closed triangles).

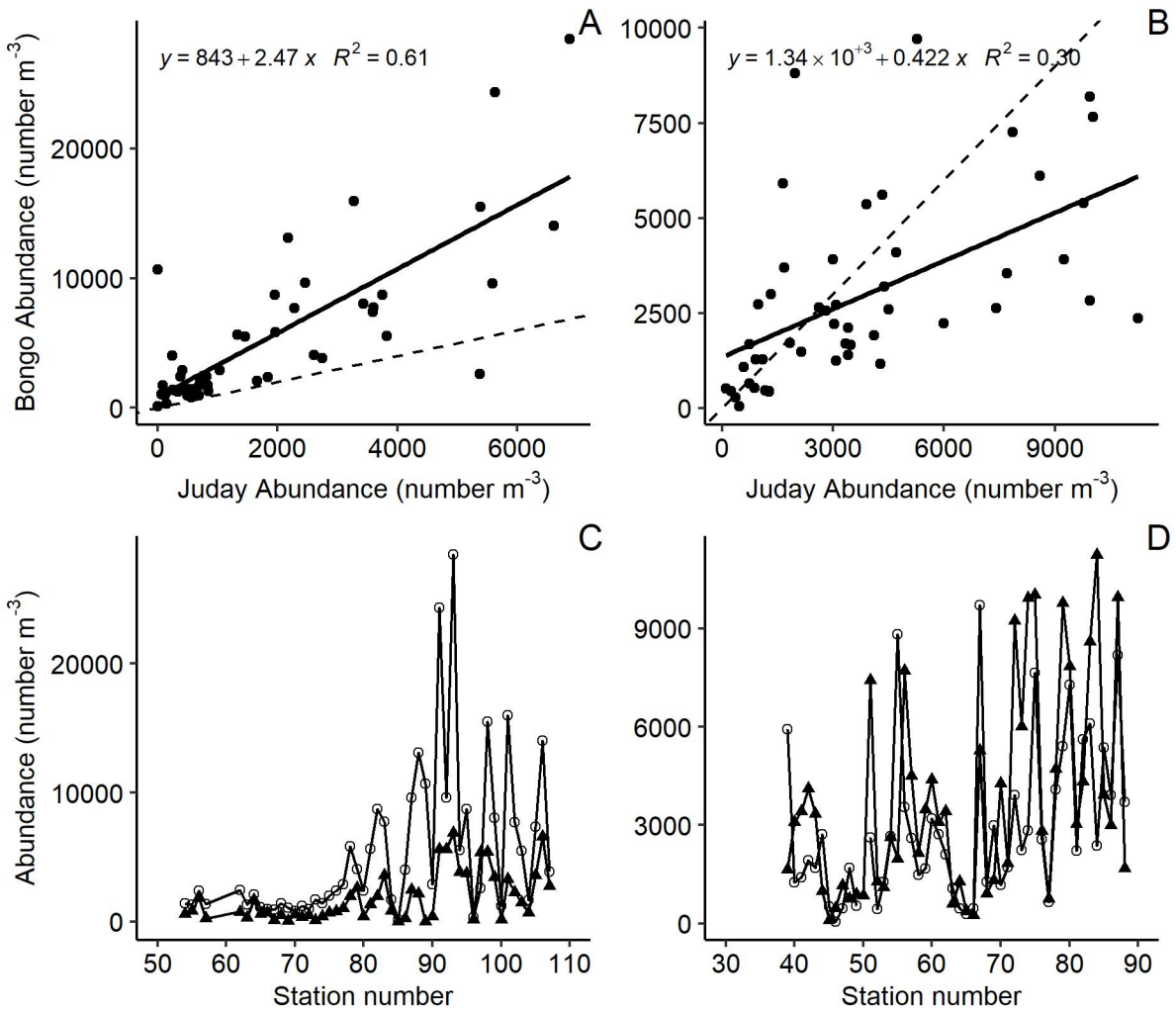

Figure S6. Comparison of *Oithona* spp. abundances between Juday and bongo nets. Linear regression fit (solid line) between the bongo and Juday net abundances for 2017 (A) and 2019 (B). Dashed line is the 1:1 line. Comparison of station by station abundances for bongo net (open circles) and vertically towed Juday net (closed triangles).

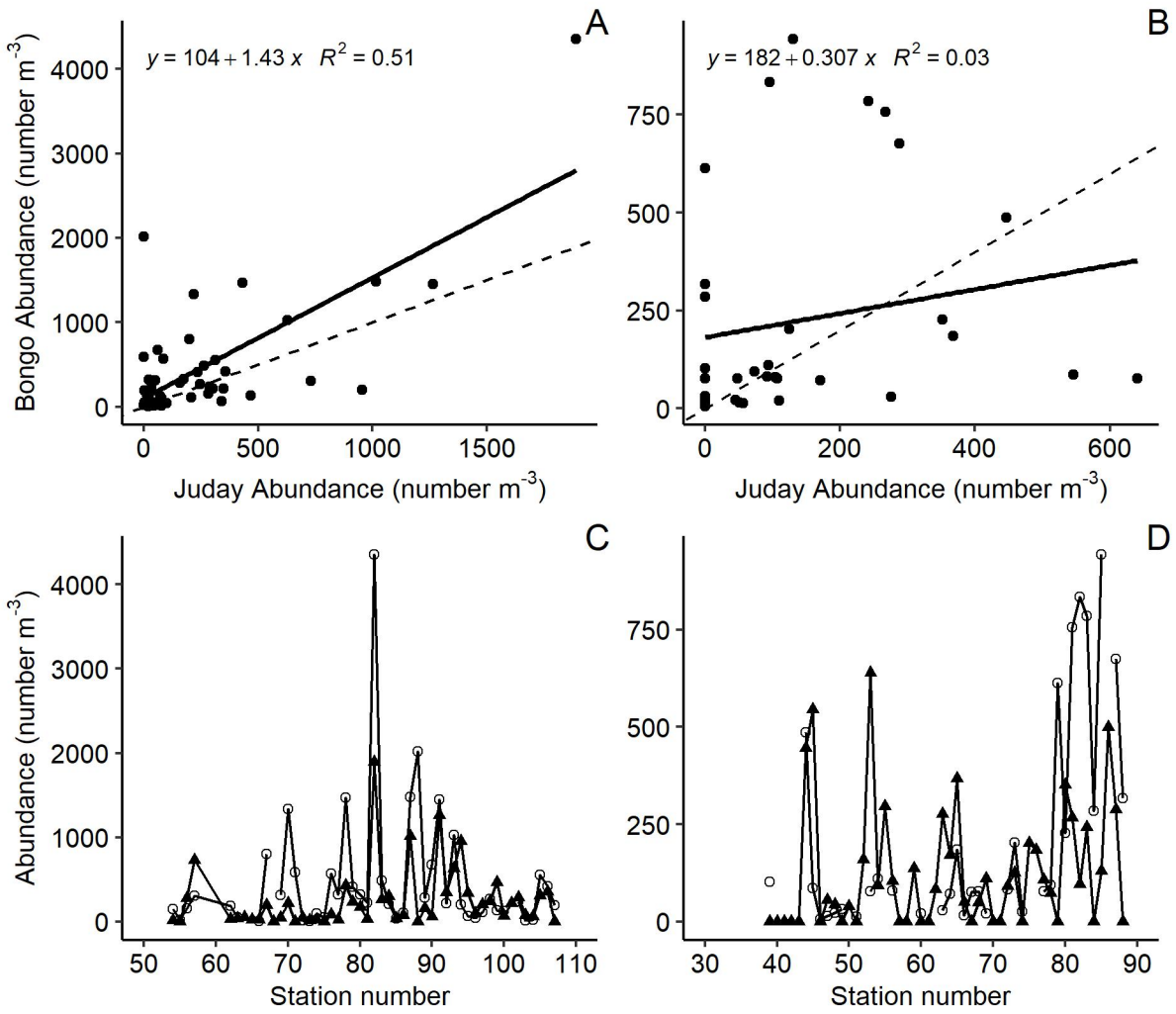

Figure S7. Comparison of Polychaeta larvae abundances between Juday and bongo nets. Linear regression fit (solid line) between the bongo and Juday net abundances for 2017 (A) and 2019 (B). Dashed line is the 1:1 line. Comparison of station by station abundances for bongo net (open circles) and vertically towed Juday net (closed triangles).

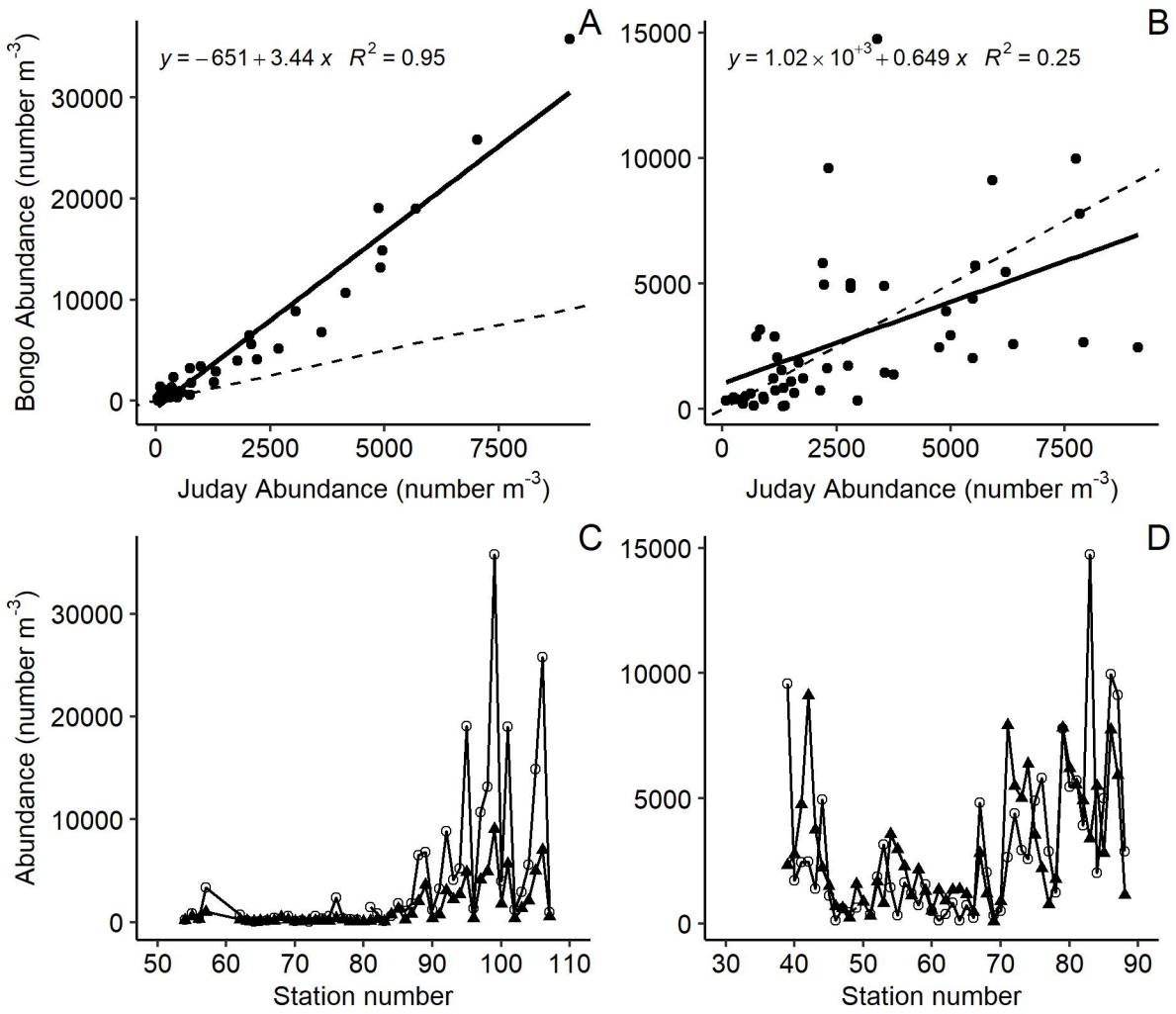

Figure S8. Comparison of *Pseudocalanus* spp. abundances between Juday and bongo nets. Linear regression fit (solid line) between the bongo and Juday net abundances for 2017 (A) and 2019 (B). Dashed line is the 1:1 line. Comparison of station by station abundances for bongo net (open circles) and vertically towed Juday net (closed triangles).

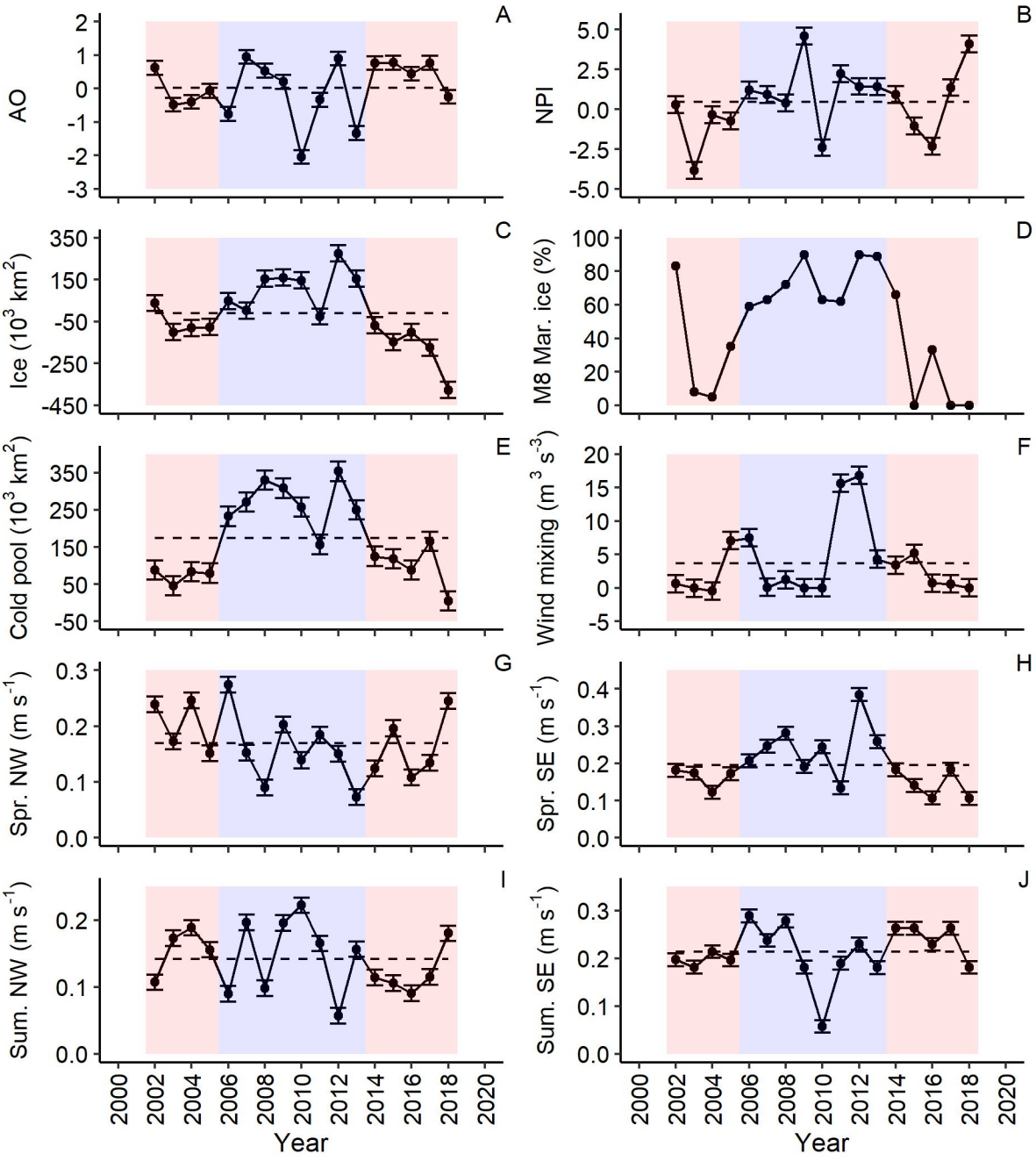

Figure S9. Annual time-series: Arctic Oscillation (AO) index (A) and North Pacific (NP) index (B) for November-March, ice area for the entire Bering Sea (C), March percent ice cover around M8 mooring (D), and cold pool area (E). Wind mixing (June-September) (F), Northwest (NW) (G) and southeast (SE) (H) wind speed for spring (February-May), NW (I) and SE (J) wind speed for summer (June-September). Plots are shaded red for warm years (2002-2005; 2014-2018) and blue for cold years (2006-2013). Error bars are standard error of the mean and dashed line represents the time-series mean (2002-2018).

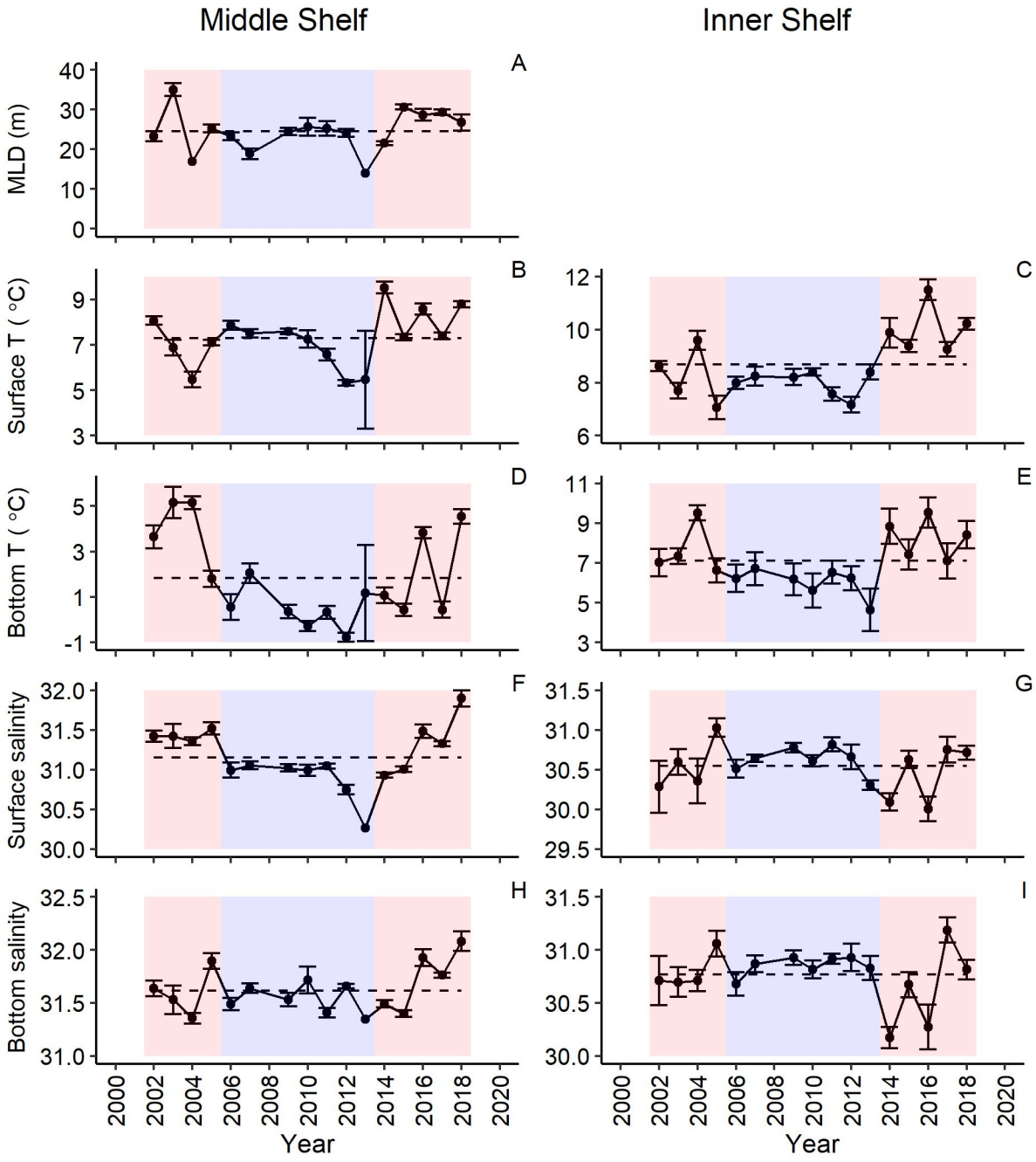

Figure S10. Annual time-series: Mixed layer depth (MLD) (A, middle shelf only); surface temperature (T) (B, C), bottom temperature (T) (D, E) surface salinity (F, G), and bottom salinity (H, I) for the middle (left panels) and inner shelf (right panels). Plots are shaded red for warm years (2002-2005; 2014-2018) and blue for cold years (2006-2013). Error bars are standard error of the mean and dashed line represents the time-series mean (2002-2018).

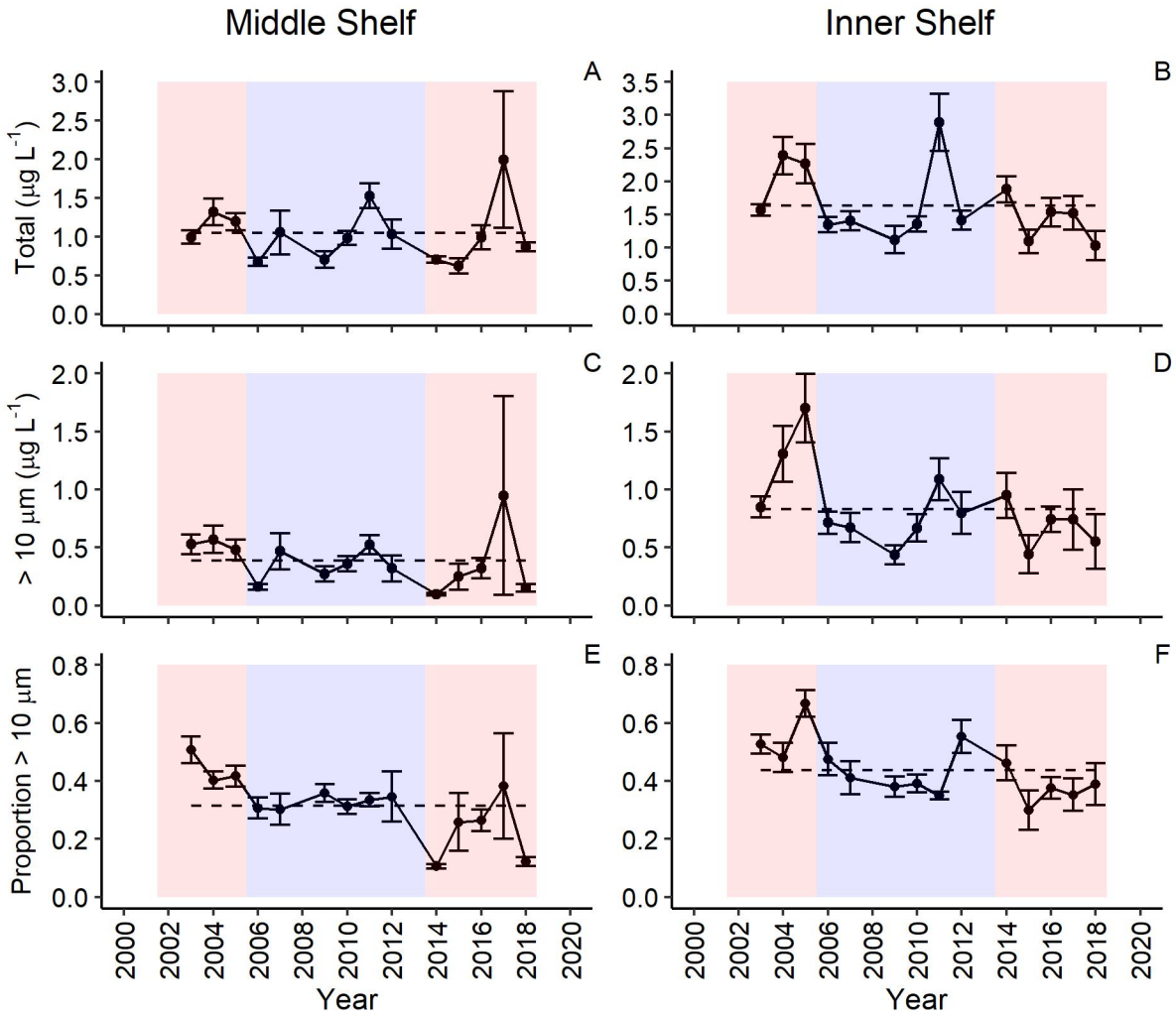

Figure S11. Annual time-series: Total chlorophyll *a* concentration (Total) (A, B), Chlorophyll *a* > 10 µm cell diameter concentration (> 10 µm) (C, D), and proportion of chlorophyll *a* > 10 µm (E, F) for the middle (left panels) and inner shelf (right panels). Plots are shaded red for warm years (2002-2005; 2014-2018) and blue for cold years (2006-2013). Error bars are standard error of the mean and dashed line represents the time-series mean (2002-2018).

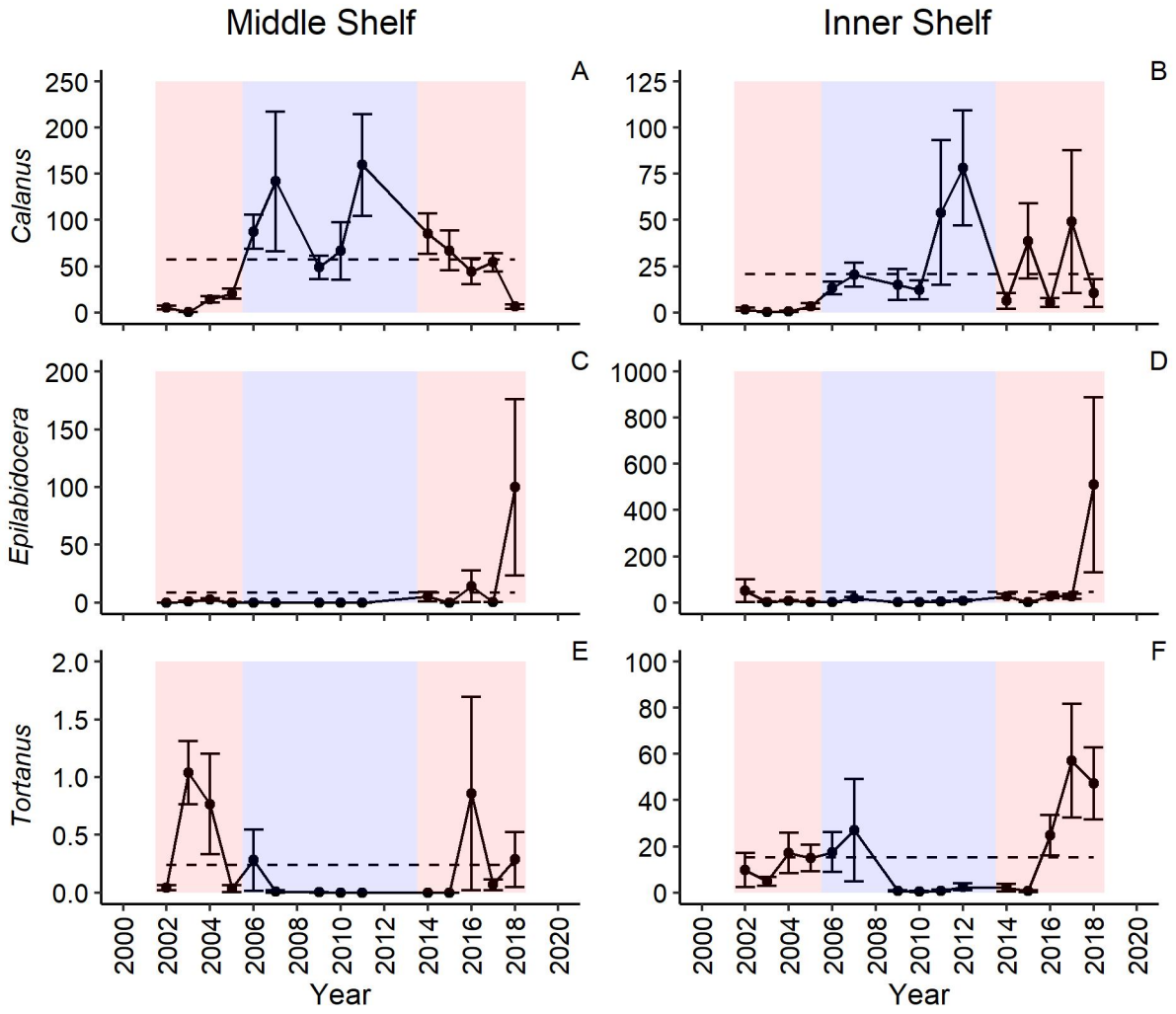

Figure S12. Annual time-series of abundance (individuals m^{-3}) for Copepods > 2 mm: *Calanus* spp. (A, B), *Epilabidocera longipedata* (C, D), and *Tortanus discaudatus* (E, F) for the middle (left panels) and inner shelf (right panels). Plots are shaded red for warm years (2002-2005; 2014-2018) and blue for cold years (2006-2013). Error bars are standard error of the mean and dashed line represents the time-series mean (2002-2018).

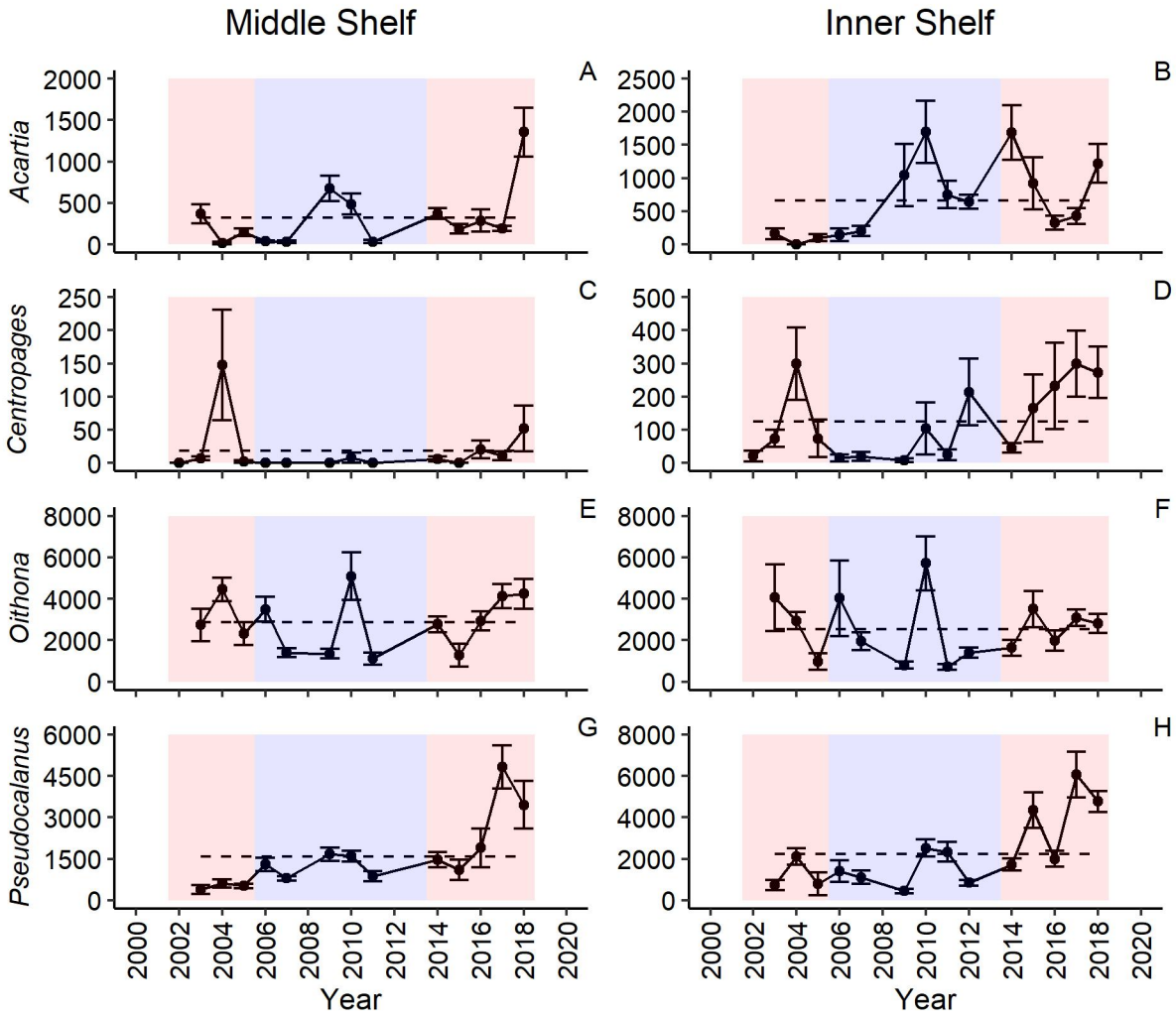

Figure S13. Annual time-series of abundance (individuals m^{-3}) for Copepods < 2 mm: *Acartia* spp. (A, B), *Centropages abdominalis* (C, D), and *Oithona* spp. (E, F), and *Pseudocalanus* spp. (G, H) for the middle (left panels) and inner shelf (right panels). Plots are shaded red for warm years (2002-2005; 2014-2018) and blue for cold years (2006-2013). Error bars are standard error of the mean and dashed line represents the time-series mean (2002-2018).

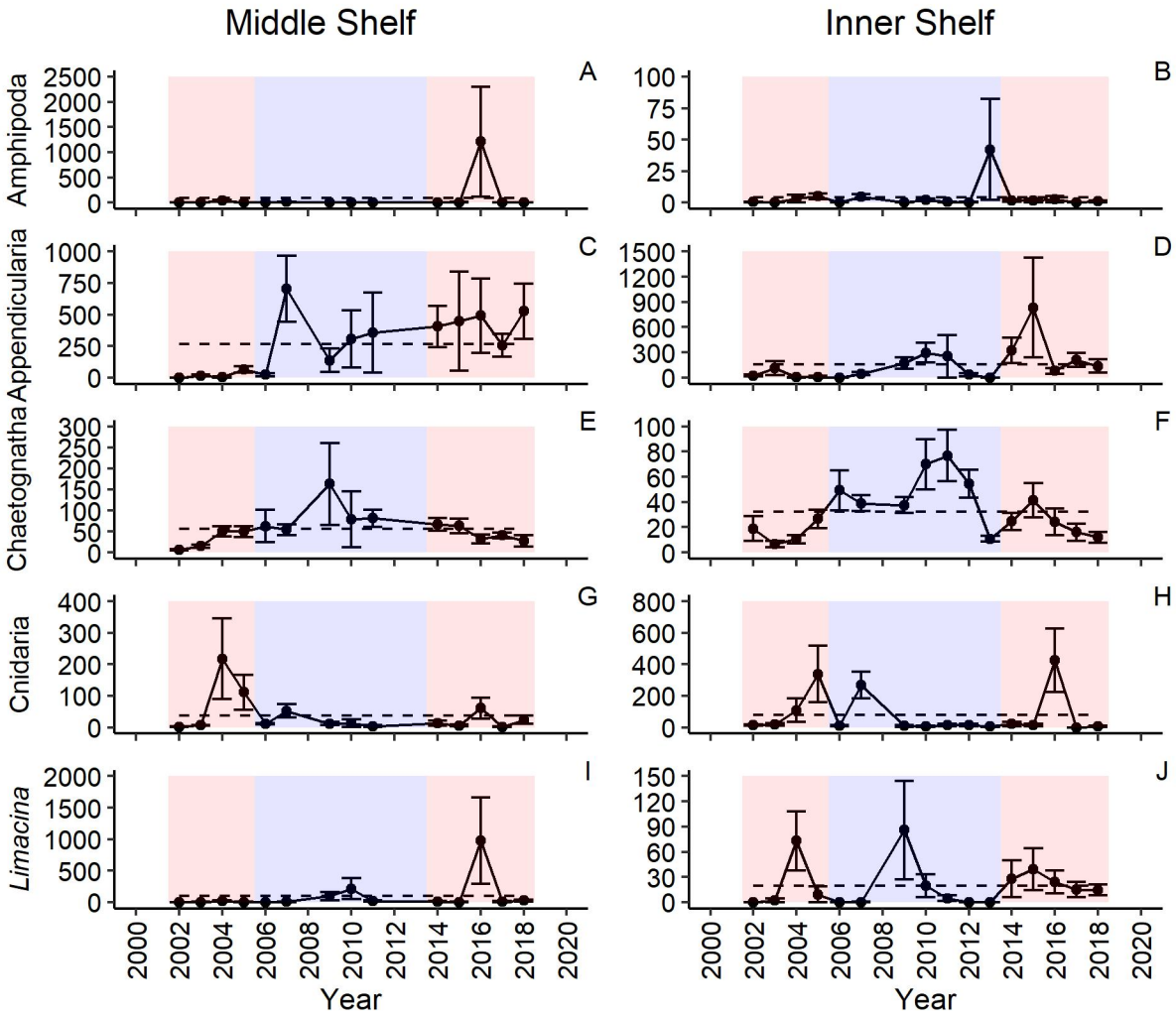

Figure S14. Annual time-series of abundance (individuals m^{-3}) for Other Holoplankton. Amphipoda (A, B), Appendicularia (C, D), Chaetognatha (E, F), Cnidaria (G, H), and *Limacina helicina*. (I, J) for the middle (left panels) and inner shelf (right panels). Plots are shaded red for warm years (2002-2005; 2014-2018) and blue for cold years (2006-2013). Error bars are standard error of the mean and dashed line represents the time-series mean (2002-2018).

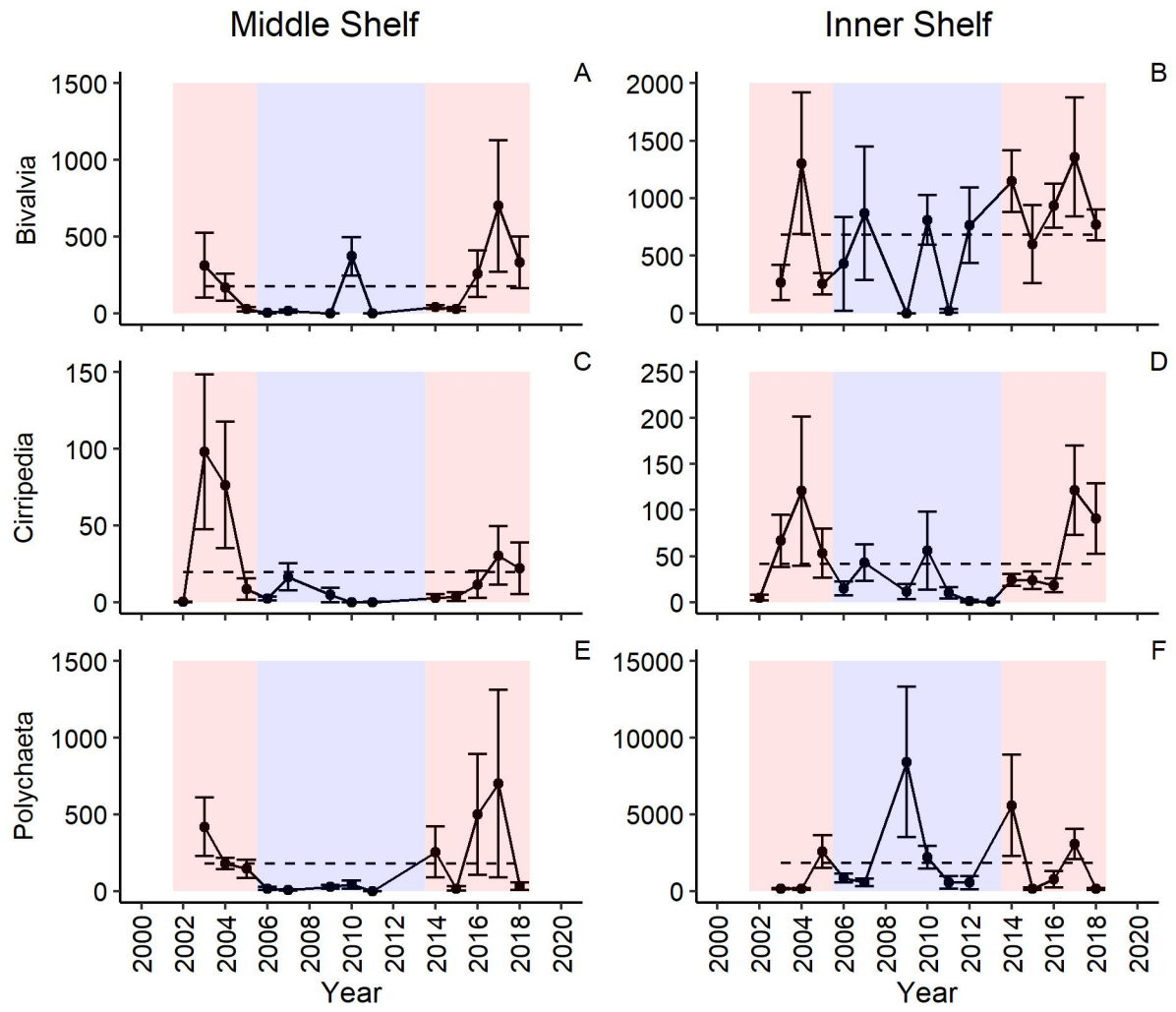

Figure S15. Annual time-series of abundance (individuals m^{-3}) for Meroplankton: Bivalvia (A, B), Cirripedia (C, D), Polychaeta (E, F) for the middle (left panels) and inner shelf (right panels). Plots are shaded red for warm years (2002-2005; 2014-2018) and blue for cold years (2006-2013). Error bars are standard error of the mean and dashed line represents the time-series mean (2002-2018).